An Error Model of a Complementary Filter for use in Bayesian Estimation - The CF-EKF Filter

Leandro R. Lustosa * **Sergio Pizziol** * **François Defaÿ** * **Jean-Marc Moschetta** *

* *Institut Supérieur de l'Aéronautique et de l'Espace (ISAE), Toulouse, 31400 France (e-mail: {leandro-ribeiro.lustosa, sergio.pizziol, francois.defay, jean-marc.moschetta} @isae.fr).*

Abstract: It is well known that stand-alone inertial navigation systems (INS) have their errors diverging with time. Consequently, an upper bound on the duration of INS systems precludes their use in low-cost micro unmanned aerial vehicles. The traditional approach for solving this matter is to resort to aiding devices, e.g., global navigation satellite system (GNSS) receivers, sighting devices, etc. Two philosophies have been extensively applied to perform data fusion: extended Kalman filtering (EKF) and complementary filtering (CF). Previous work in the literature showed that the computationally less expensive CF can be robustly applied to attitude estimation using low-cost sensors and achieve performance that is comparable to that of a full EKF. However, performance is degraded by vehicle manoeuvres and no measurement on estimate uncertainties is given. Furthermore, a large number of sensors makes it impracticable for optimal tuning of the CF. The present work lays the foundation for sensor filtering that employs the CF for attitude estimation by means of a magnetometer as an external aid, and an EKF for additional sensors integration. The main feature of this architecture is the possibility of deployment in a distributed multi-platform system and implementation of fault isolation by running the CF stage in a separate low-throughput reliable machine for stand-alone degraded mode operation. A case study is performed on synthetic data from inertial, magnetic and GNSS sensors.

Keywords: Sensor data fusion; filtering, estimation; UAV navigation, guidance and control.

1. INTRODUCTION

The dead-reckoning nature of stand-alone inertial navigation systems (INS) impose cumulative errors in the estimation of position, velocity and attitude. Consequently, an upper bound on the duration of stand-alone INS systems precludes their use in low-cost or micro unmanned aerial vehicles (μUAV). The traditional approach for solving such inconvenience is to resort to aiding devices such as global navigation satellite system (GNSS) receivers, magnetometers and/or sighting devices. Two philosophies have been extensively applied to perform this data fusion: extended Kalman filtering (EKF) and complementary filtering (CF).

Some key similarities and differences between EKF and CF are discussed in [Higgins (1975)]. For instance, a CF is equivalent to an EKF under steady-state conditions. However, navigation errors dynamics and observability are dependent on vehicle trajectory [Goshen-Meskin and Bar-Itzhack (1992)] in such a way that an EKF can outperform a CF in manoeuvring conditions. Be that as it may, the use of low-cost sensors renders the EKF suboptimal and often inconsistent due to large navigation error covariances that undermine linearization assumptions. Particle filters [Gordon et al. (1993)] have been employed to solve such problem but require a fair amount of computational power often not available in low-cost or micro-UAVs applications. CF, on the other hand, is an exceptionally inexpensive filter.

Previous work [Euston et al. (2008)] has shown that the CF can be robustly applied to low-cost sensors and achieve performance that is comparable to that of a full suboptimal EKF based on GNSS-aided inertial measurement unit (IMU/GNSS) when vehicle dynamics is taken into consideration by means of airspeed measurements. Another strategy to relax the CF required assumption of constant velocity motion is to apply gains that adapt to the motion to be estimated [Calusdian et al. (2011)]. The issue of tuning a given CF is discussed in detail in [Vasconcelos et al. (2009)] to shape a frequency response that blends the frequency contents of the aiding devices and the inertial sensors (implementation aspects are also highlighted). [Mahony et al. (2005)] compares two implementation architectures for the CF, namely, direct CF and passive CF, and shows that the latter has superior dynamical properties, proves its convergence and extends it to provide adaptive rate-gyro drift estimation.

The present work exploits the passive CF for position, velocity and attitude estimation employing a magnetometer as an external aid to bound attitude errors. On top

⋆ This work is partially supported by the Conselho Nacional de Desenvolvimento Científico e Tecnológico, CNPq.

of that, an external EKF is applied to restrain position and velocity errors by means of GNSS measurements. To the authors' knowledge, there is no previous work on how to seamlessly connect both filters, although there are *ad hoc* CF-EKF filter interconnection and tuning [Jung and Tsiotras (2007)]. This paper contributes by delineating the overall CF-EKF filter structure designed to simplify the tedious tuning process, studying some of its properties and delivering implementation details. Furthermore, some EKF aiding devices (sighting devices, for instance) call for operational systems that increases system complexity thus reducing INS reliability. In view of this, it is shown how to effectively employ CF-EKF in a multi-platform UAV to implement fault isolation by running the CF stage in a separate low-throughput low-level reliable machine for stand-alone degraded mode operation.

In the following, an attitude passive CF based on gravitational and magnetic fields is reviewed (section 3.1) and its dynamic properties are discussed (section 3.3). Moreover, this work contributes by delivering an error model of this complementary filter based on psi-angle representation (section 3.2) for statistical error analysis and extended Kalman or information filter integration (section 4). The proposed framework is evaluated by means of a distributed loosely-coupled IMU/GNSS Kalman filter applied to synthetic IMU/GNSS sensor data (section 5). Finally, concluding remarks and perspectives are presented (section 6).

2. NOTATION AND REFERENCE FRAMES

In this paper, kinematic quantities of interest in multiple moving reference frames are algebraically studied and, accordingly, a consistent and precise notation is called for. Therefore, this section states the notation conventions applied herein, including relevant reference frames definition and related variables of interest.

The notation ${}^a\boldsymbol{x}^c$ is employed, where the symbol x is replaced by the symbol of the desired vector quantity (p for position, v for velocity, a for acceleration, ω for angular velocity) of frame/point (depending on the context) C with respect to frame A. For instance, ${}^i\boldsymbol{\omega}^b$ denotes angular velocity of frame B with respect to frame I.

The decomposition of a vector $\boldsymbol{x} \in \mathbb{R}^n$ into its components in a coordinate system R is denoted by means of the right subscript position, e.g.

$$\boldsymbol{x}_r = (x_{r1}\ x_{r2}\ \cdots\ x_{rn})^T \tag{1}$$

We make extensive use of the vector product operation and its matrix representation (in some basis B) is denoted by

$$\boldsymbol{v}_b\times = [\boldsymbol{v}_b\times] = \begin{bmatrix} 0 & -v_{b3} & v_{b2} \\ v_{b3} & 0 & -v_{b1} \\ -v_{b2} & v_{b1} & 0 \end{bmatrix} \tag{2}$$

Quaternion algebra structure definition varies to a small extent in literature, but herein a quaternion $q \in (\mathbb{R}^4, \times)$ is defined as [Stevens and Lewis (2003)]

$$q = \begin{pmatrix} q_0 \\ \boldsymbol{q} \end{pmatrix} \tag{3}$$

where $q_0 \in \mathbb{R}$ and $\boldsymbol{q} \in \mathbb{R}^3$ with quaternion product operation defined as

$$p \times q = \begin{pmatrix} p_0 q_0 - \boldsymbol{p}\cdot\boldsymbol{q} \\ p_0\boldsymbol{q} + q_0\boldsymbol{p} + \boldsymbol{p}\times\boldsymbol{q} \end{pmatrix} \tag{4}$$

The quaternion and direction cosine matrix (DCM) representations of rotation from frame A to B, respectively q_b^a and D_b^a, are defined in the direction such that the rotation formulas [Stevens and Lewis (2003)] are written as

$$\begin{pmatrix} 0 \\ \boldsymbol{x}_b \end{pmatrix} = (q_b^a)' \times \begin{pmatrix} 0 \\ \boldsymbol{x}_a \end{pmatrix} \times q_b^a \tag{5}$$

and

$$\boldsymbol{x}_b = D_b^a \boldsymbol{x}_a \tag{6}$$

where $(q_b^a)'$ is the quaternion conjugate of q_b^a.

The low-cost strapdown inertial navigation nature of the filter motivates the definition of the three reference frames illustrated in figure 1.

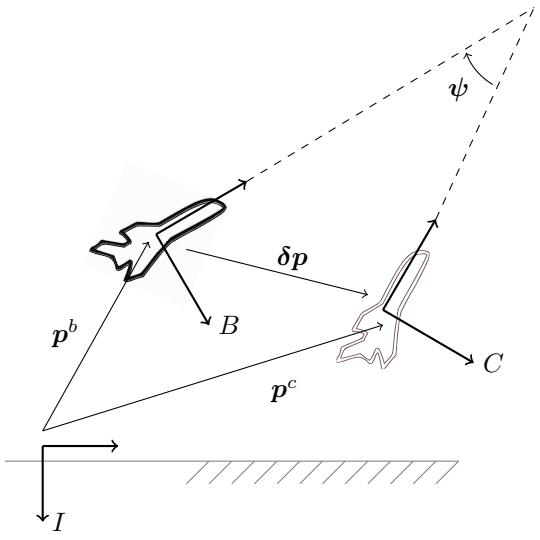

Fig. 1. Reference frames illustration. The inertial (I), body (B) and computed (C) frames are fixed to the Earth, IMU and estimated orientation by the attitude complementary filter, respectively.

The *inertial frame* I is assumed stationary with respect to Earth since this work targets low-cost sensors that possess low rate-gyro precision when compared to Earth angular velocity order-of-magnitude. On the other hand, the *body axes* B are fixed in the inertial measurement unit (IMU) and yields a natural vector space basis for sensor measurements. Finally, an embedded processor collects sensor data and computes IMU position and attitude with respect to I by means of the attitude complementary filter (see section 3). Due to sensors errors, the estimated orientation of B is misaligned and it is denoted by the *computed frame* C.

3. ATTITUDE COMPLEMENTARY FILTER

3.1 Filter description

This section reviews an attitude complementary filter that, when applied to rate-gyro, accelerometer and magnetometer measurements, yields attitude estimation with bounded errors (see figure 2). Additionally, it delivers position and velocity estimators. However, their errors grow

with time and call for additional sensors and data fusion algorithms (see section 4).

Fig. 2. Input-output schematic view of the quaternion complementary filter.

This work models the rate-gyro measurement $\boldsymbol{\omega}(t)$ as a superposition of the nominal value ${}^i\boldsymbol{\omega}_b^b(t)$, a random constant (with respect to body axes) Gaussian drift $\boldsymbol{\varepsilon}_b \sim N(\mathbf{0}, \Sigma_\varepsilon)$ and white Gaussian noise $\boldsymbol{\nu}_b^g(t) \sim N(\mathbf{0}, \Sigma_g)$ such that

$$\boldsymbol{\omega}(t) = {}^i\boldsymbol{\omega}_b^b(t) + \boldsymbol{\varepsilon}_b + \boldsymbol{\nu}_b^g(t) \tag{7}$$

Similarly, accelerometer and magnetometer measurements, $\boldsymbol{f}(t)$ and $\boldsymbol{b}(t)$, respectively, are modeled as

$$\boldsymbol{f}(t) = {}^i\boldsymbol{a}_b^b(t) - \boldsymbol{g}_b(t) + \boldsymbol{\nabla}_b + \boldsymbol{\nu}_b^a(t) \tag{8}$$

and

$$\boldsymbol{b}(t) = \boldsymbol{B}_b(t) + \boldsymbol{\Delta}_b + \boldsymbol{\nu}_b^m(t) \tag{9}$$

where $\boldsymbol{\nabla}_b \sim N(\mathbf{0}, \Sigma_\nabla)$, $\boldsymbol{\nu}_b^a(t) \sim N(\mathbf{0}, \Sigma_a)$, $\boldsymbol{\Delta}_b \sim N(\mathbf{0}, \Sigma_\Delta)$, $\boldsymbol{\nu}_b^m(t) \sim N(\mathbf{0}, \Sigma_m)$, and $\boldsymbol{g}$ denote, respectively, accelerometer/magnetometer bias/noise, and Earth gravitational acceleration.

Notice that direct integration of equation 7 yields attitude estimators with unbounded errors that call for additional sensors. The present version of the attitude complementary filter assumes the local magnetic field $\boldsymbol{B}_i$ is known and compares a predicted measure $\boldsymbol{B}_c$ with an ideal measure $\boldsymbol{B}_b$ to produce a residual that should be closely related to attitude errors. Mathematically, notice that

$$\boldsymbol{B}_b \times \boldsymbol{B}_c = -[\boldsymbol{B}_c\times]\boldsymbol{B}_b = -[\boldsymbol{B}_c\times]D_b^c\boldsymbol{B}_c \tag{10}$$

where D_b^c is the DCM that transforms computed frame coordinates into body axes components. Assuming a $3-2-1$ rotation order of ψ_3, ψ_2 and ψ_1, respectively, D_b^c can be written as

$$D_b^c = \begin{bmatrix} c\psi_2 c\psi_3 & c\psi_2 s\psi_3 & -s\psi_2 \\ s\psi_1 s\psi_2 c\psi_3 - c\psi_1 s\psi_3 & c\psi_1 c\psi_3 + s\psi_1 s\psi_2 s\psi_3 & s\psi_1 c\psi_2 \\ s\psi_1 s\psi_3 + c\psi_1 s\psi_2 c\psi_3 & c\psi_1 s\psi_2 s\psi_3 - s\psi_1 c\psi_3 & c\psi_1 c\psi_2 \end{bmatrix} \tag{11}$$

If small error angles ψ_i are assumed, $cos\psi_i \to 1$, $sin\psi_i \to \psi_i$, and equation 11 is simplified to

$$D_b^c = \begin{bmatrix} 1 & \psi_3 & -\psi_2 \\ -\psi_3 & 1 & \psi_1 \\ \psi_2 & -\psi_1 & 1 \end{bmatrix} = I - [\boldsymbol{\psi}\times] \tag{12}$$

where

$$\boldsymbol{\psi} = \begin{pmatrix} \psi_1 & \psi_2 & \psi_3 \end{pmatrix}^T \tag{13}$$

Therefore, equation 10 can be simplified to read

$$\boldsymbol{B}_b \times \boldsymbol{B}_c = -[\boldsymbol{B}_c\times](I - [\boldsymbol{\psi}\times])\boldsymbol{B}_c = -[\boldsymbol{B}_c\times]^2\boldsymbol{\psi} \tag{14}$$

Assuming the local gravitational vector is known, a similar development yields

$$\boldsymbol{g}_b \times \boldsymbol{g}_c = -[\boldsymbol{g}_c\times]^2\boldsymbol{\psi} \tag{15}$$

Equations 14 and 15 contain candidates for feedback stabilization of $\boldsymbol{\psi}$ as a consequence of their proportionality to $\boldsymbol{\psi}$. Accordingly, an estimator ${}^i\boldsymbol{\omega}_c^c$ for ${}^i\boldsymbol{\omega}_b^b$, namely, the angular velocity of the body reference frame with respect to the inertial frame described in the body axes, is defined as

$${}^i\boldsymbol{\omega}_c^c = \boldsymbol{\omega} - k_a\boldsymbol{f} \times \boldsymbol{g}_c + k_m\boldsymbol{b} \times \boldsymbol{B}_c \tag{16}$$

where $k_a, k_m > 0$. From the embedded processor point of view, equation 16 can be computed as

$${}^i\boldsymbol{\omega}_c^c = \boldsymbol{\omega} - k_a\boldsymbol{f} \times D_c^i\boldsymbol{g}_i + k_m\boldsymbol{b} \times D_c^i\boldsymbol{B}_i \tag{17}$$

where D_c^i is computed by means of q_c^i, which can be numerically computed from the following classic [Stevens and Lewis (2003)] quaternion differential equation

$$\frac{d}{dt}q_c^i = \frac{1}{2}\begin{bmatrix} 0 & -({}^i\boldsymbol{\omega}_c^c)^T \\ {}^i\boldsymbol{\omega}_c^c & -[{}^i\boldsymbol{\omega}_c^c\times] \end{bmatrix} q_c^i \tag{18}$$

and quaternion to DCM transformation equation

$$D_c^i = \begin{bmatrix} (1-2q_2^2-2q_3^2) & 2(q_1q_2+q_0q_3) & 2(q_1q_3-q_0q_2) \\ 2(q_1q_2-q_0q_3) & (1-2q_1^2-2q_3^2) & 2(q_2q_3+q_0q_1) \\ 2(q_1q_3+q_0q_2) & 2(q_2q_3-q_0q_1) & (1-2q_1^2-2q_2^2) \end{bmatrix} \tag{19}$$

Finally, position and velocity estimators are obtained by means of direct integration of the following mechanization equations

$$\frac{d}{dt}\boldsymbol{p}_i^c = {}^i\boldsymbol{v}_i^c \tag{20}$$

and

$$\frac{d}{dt}{}^i\boldsymbol{v}_i^c = D_i^c\boldsymbol{f} + \boldsymbol{g}_i \tag{21}$$

Equations 17, 18, 19, 20 and 21 implement the CF inertial navigation algorithm of figure 2. In the next two subsections, some of its properties are re-derived in view of the misalignment model, which is the main contribution of this work and the necessary foundation for CF-EKF interfacing.

3.2 Complementary filter misalignment error model

This section develops an error model for $\boldsymbol{\psi}(t)$, i.e., a stochastic differential equation that models complementary filter inertial navigation errors in time due to vehicle motion and uncertainties in sensors.

Initially, notice that $\boldsymbol{\psi}(t)$ is composed by Euler angles and their relation to angular velocity is dictated by [Stevens and Lewis (2003)]

$$\frac{d}{dt}\boldsymbol{\psi} = \begin{bmatrix} 1 & \tan\psi_2\sin\psi_1 & \tan\psi_2\cos\psi_1 \\ 0 & \cos\psi_1 & -\sin\psi_1 \\ 0 & \dfrac{\sin\psi_1}{\cos\psi_2} & \dfrac{\cos\psi_1}{\cos\psi_2} \end{bmatrix} {}^c\boldsymbol{\omega}_b^b \tag{22}$$

Assuming small angles and gathering only first order terms, we can write

$$\frac{d}{dt}\boldsymbol{\psi} = {}^c\boldsymbol{\omega}_b^b \tag{23}$$

so that

$$\frac{d}{dt}\boldsymbol{\psi} = {}^i\boldsymbol{\omega}_b^b - {}^i\boldsymbol{\omega}_b^c = {}^i\boldsymbol{\omega}_b^b - D_b^c \cdot {}^i\boldsymbol{\omega}_c^c = {}^i\boldsymbol{\omega}_b^b - {}^i\boldsymbol{\omega}_c^c + [\boldsymbol{\psi}\times]{}^i\boldsymbol{\omega}_c^c \tag{24}$$

by means of equation 12. Therefore,

$${}^i\boldsymbol{\omega}_b^b - {}^i\boldsymbol{\omega}_c^c = \frac{d}{dt}\boldsymbol{\psi} + [{}^i\boldsymbol{\omega}_c^c\times]\boldsymbol{\psi} \tag{25}$$

Substituting equations 7, 8, 16 into 25, we obtain

$$\begin{aligned}\frac{d\boldsymbol{\psi}}{dt} = &\Big(-[{}^i\boldsymbol{\omega}_c^c\times] + k_m[\boldsymbol{B}_c\times]^2 + k_a[\boldsymbol{g}_c\times]^2\Big)\boldsymbol{\psi} + \\ &+ \Big(-I\Big)\boldsymbol{\varepsilon}_b + \Big(-k_a[\boldsymbol{g}_c\times]\Big)\boldsymbol{\nabla}_b + \Big(k_m[\boldsymbol{B}_c\times]\Big)\boldsymbol{\Delta}_b + \\ &+ \Big(-I\Big)\boldsymbol{\nu}_b^g + \Big(k_m[\boldsymbol{B}_c\times]\Big)\boldsymbol{\nu}_b^m + \Big(-k_a[\boldsymbol{g}_c\times]\Big)\boldsymbol{\nu}_b^a + \\ &+ \Big(-k_a[\boldsymbol{g}_c\times]\Big){}^i\boldsymbol{a}_b^b \quad (26)\end{aligned}$$

On the other hand, the errors on position and velocity, namely,

$$\boldsymbol{\delta p} \triangleq \boldsymbol{p}^c - \boldsymbol{p}^b \quad (27)$$

and

$$\boldsymbol{\delta v} \triangleq {}^i\boldsymbol{v}^c - {}^i\boldsymbol{v}^b \quad (28)$$

have the following well-known differential equations for their time evolution [Bar-Shalom et al. (2001)]

$$\frac{d}{dt}\boldsymbol{\delta p}_i = \boldsymbol{\delta v}_i \quad (29)$$

and

$$\frac{d}{dt}\boldsymbol{\delta v}_i = D_i^c[\boldsymbol{f}\times]\boldsymbol{\psi} + D_i^c\boldsymbol{\nabla}_b + D_i^c\boldsymbol{\nu}_b^a \quad (30)$$

Equations 26, 29 and 30 describe errors stochastic time evolution in the CF inertial navigation algorithm and can be used for several purposes, e.g., algorithm stability analysis (subsection 3.3) and Kalman filtering data fusion (section 4).

3.3 Convergence analysis

Given sensors noise and bias characteristics, equation 26 provides the means to statistically predict the performance of the CF (for small $\boldsymbol{\psi}$). Furthermore, it describes the dynamics of the attitude estimation error $\boldsymbol{\psi}(t)$. Considering bias and noise quantities as filter inputs, the local stability of the attitude CF is determined by the following linear time-variant system

$$\frac{d\boldsymbol{\psi}}{dt} = \underbrace{\Big(-[{}^i\boldsymbol{\omega}_c^c\times] + k_m[\boldsymbol{B}_c\times]^2 + k_a[\boldsymbol{g}_c\times]^2\Big)}_{N}\boldsymbol{\psi} \quad (31)$$

Although $\boldsymbol{\psi}$ has no physical meaningful basis (among other, rotations do not have a vector space structure), one can assign a basis to $\boldsymbol{\psi}$ and treat it as if it was a vector algebraically. Since equation 31 is fully described in computed basis, we assign the C basis to $\boldsymbol{\psi}$ such that

$$\frac{d\boldsymbol{\psi}_c}{dt} + [{}^i\boldsymbol{\omega}_c^c\times]\boldsymbol{\psi}_c = \Big(k_m[\boldsymbol{B}_c\times]^2 + k_a[\boldsymbol{g}_c\times]^2\Big)\boldsymbol{\psi}_c \quad (32)$$

The reasoning that transformed equation 31 into 32 is subtle but allows one to evoke the transport theorem from classical mechanics and rewrite the left-hand side as

$$\Big(\frac{d\boldsymbol{\psi}_i}{dt}\Big)_c = \Big(k_m[\boldsymbol{B}_c\times]^2 + k_a[\boldsymbol{g}_c\times]^2\Big)\boldsymbol{\psi}_c \quad (33)$$

such that

$$\frac{d\boldsymbol{\psi}_i}{dt} = D_i^c\underbrace{\Big(k_m[\boldsymbol{B}_c\times]^2 + k_a[\boldsymbol{g}_c\times]^2\Big)}_{M}D_c^i\boldsymbol{\psi}_i \quad (34)$$

The interested reader can quickly check that every matrix of the form $[\boldsymbol{v}\times]^2$ has eigenvalues $\lambda_1 = 0$, with algebraic multiplicity 1, and $\lambda_2 = -|\boldsymbol{v}|^2$ with algebraic multiplicity 2. Therefore, M is a linear combination of such matrices and it is negative semi-definite if $k_m > 0$ and $k_a > 0$. Therefore, the CF filter is marginally stable [1] for attitude determination.

Position and velocity estimation errors, on the other hand, remains unbounded and call for additional sensors, which are commonly integrated by means of Kalman filters. The next section provides a clean strategy to easily integrate and tune an EKF on top of a complementary filter.

4. KALMAN FILTER INTEGRATION

In the light of the foregoing development, it is convenient to define the EKF state vector as

$$\boldsymbol{x} = \begin{pmatrix}\boldsymbol{\delta p}_i & \boldsymbol{\delta v}_i & \boldsymbol{\psi} & \boldsymbol{\nabla}_b & \boldsymbol{\varepsilon}_b & \boldsymbol{\Delta}_b\end{pmatrix}^T \quad (35)$$

and process noise as

$$\boldsymbol{w} = \begin{pmatrix}\boldsymbol{\nu}_b^a & \boldsymbol{\nu}_b^g & \boldsymbol{\nu}_b^m & {}^i\boldsymbol{a}_b^b\end{pmatrix}^T \quad (36)$$

such that

$$\dot{\boldsymbol{x}} = A\boldsymbol{x} + B\boldsymbol{w} \quad (37)$$

where A and B can be obtained by inspection of equations 26, 29 and 30, yielding

$$A = \begin{bmatrix} 0 & I & 0 & 0 & 0 & 0 \\ 0 & 0 & D_i^c[\boldsymbol{f}\times] & D_i^c & 0 & 0 \\ 0 & 0 & N & -k_a[\boldsymbol{g}_c\times] & -I & k_m[\boldsymbol{B}_c\times] \\ 0 & 0 & 0 & 0 & 0 & 0 \\ 0 & 0 & 0 & 0 & 0 & 0 \\ 0 & 0 & 0 & 0 & 0 & 0 \end{bmatrix} \quad (38)$$

and

$$B = \begin{bmatrix} 0 & 0 & 0 & 0 \\ D_i^c & 0 & 0 & 0 \\ -k_a[\boldsymbol{g}_c\times] & -I & k_m[\boldsymbol{B}_c\times] & -k_a[\boldsymbol{g}_c\times] \\ 0 & 0 & 0 & 0 \\ 0 & 0 & 0 & 0 \\ 0 & 0 & 0 & 0 \end{bmatrix} \quad (39)$$

On the other hand, the EKF observation equation is dependent on the available aiding sensors. In this paper, for illustration, a loosely-coupled GNSS receiver architecture [Farrell and Barth (1998)] is employed such that

$$\boldsymbol{y} = H\boldsymbol{x} + \boldsymbol{v} \quad (40)$$

where

$$H = \begin{bmatrix} I_{3\times3} & 0_{3\times3} & 0_{3\times12} \\ 0_{3\times3} & I_{3\times3} & 0_{3\times12} \end{bmatrix} \quad (41)$$

and $\boldsymbol{v}$ is dependent on GNSS receiver uncertainties. After discretization of equation 37, the EKF is applied (for a comprehensive discussion on Kalman filtering and useful equivalent alternative formulations for use in low-cost architectures, see [Maybeck (1979)]) and estimation of navigation errors and sensor biases is performed. After each EKF update step, the state $\boldsymbol{x}$ is used for CF correction (position, velocity and attitude feedback) and sensor on-line calibration. Figure 3 illustrates the overall architecture.

A remarkable feature of the CF-EKF is that given the statistics of the noise process defined by equation 36, one can straightforwardly tune the EKF stage by means of manufacturer sensor specs and IMU sampling rate. However, the last noise component, namely, ${}^i\boldsymbol{a}_b^b$, is rarely

[1] More precisely, it is stable except for the unlikely case when $\boldsymbol{B}$ is parallel to $\boldsymbol{g}$.

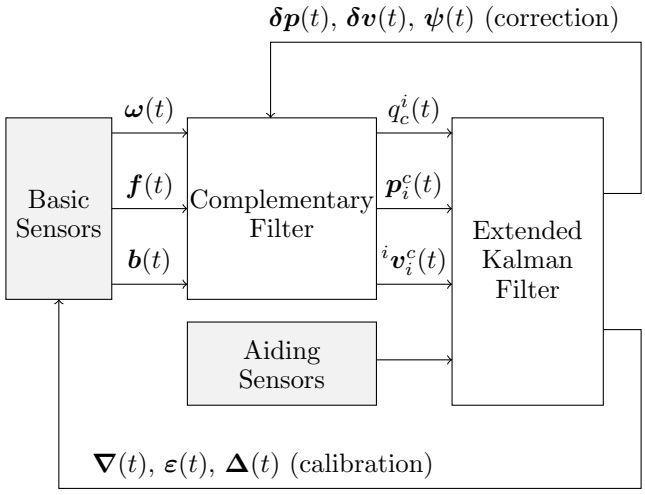

Fig. 3. CF-EKF filter overall architecture.

white nor Gaussian in reality. Therefore, it is the only noise component that might require trial-and-error tuning and careful consideration of vehicle nominal trajectories.

5. SIMULATION RESULTS

In a simulated planar circular trajectory (10m radius and $T = 60$ seconds period) with synthetic IMU/MAG/GNSS sensor data, the proposed CF-EKF filter is compared against the traditional centralized EKF and against the *ad hoc* CF/EKF filter architecture with no CF modelling compensations for a 10-run Monte Carlo simulation. Notice that the CF-EKF degenerates to the EKF when the gains k_a and k_m are set to zero. On the other hand, the *ad hoc* CF/EKF implementation is performed by setting k_a and k_m to zero only in the Kalman filter process matrices A and B (equations 38 and 39). This implies the same computed covariance matrices for both EKF and *ad hoc* implementations. Kalman filter is tuned by means of nominal sensor statistics in all three cases. Similarly, complementary gains k_a and k_m are kept constant throughout different implementations. Finally, the arbitrarily chosen orientation of the simulated vehicle is such that the yaw ψ, pitch θ and roll ϕ angles are given by

$$\psi(t) = \theta(t) = \phi(t) = \frac{2\pi}{T}t \tag{42}$$

Figures 4 and 5 represents position, velocity, misalignment, accelerometer bias, rate-gyro drift and magnetometer bias root mean square (RMS) estimation errors and their respective predicted error covariance values in function of time.

Notice that errors and covariances for position estimation are similar throughout all three implementations. In particular, the position covariance for the CF-EKF is only slightly larger than the optimal EKF. This feature illustrates the trade-off of centralized optimal and distributed sub-optimal estimation architectures. This trade-off is stronger in velocity estimation where a factor of 2 is observed between EKF and CF-EKF estimated error covariances. On the other hand, EKF and *ad hoc* CF/EKF share the same error covariance values. However, the *ad hoc* CF/EKF RMS values rise above the 3σ curve yielding

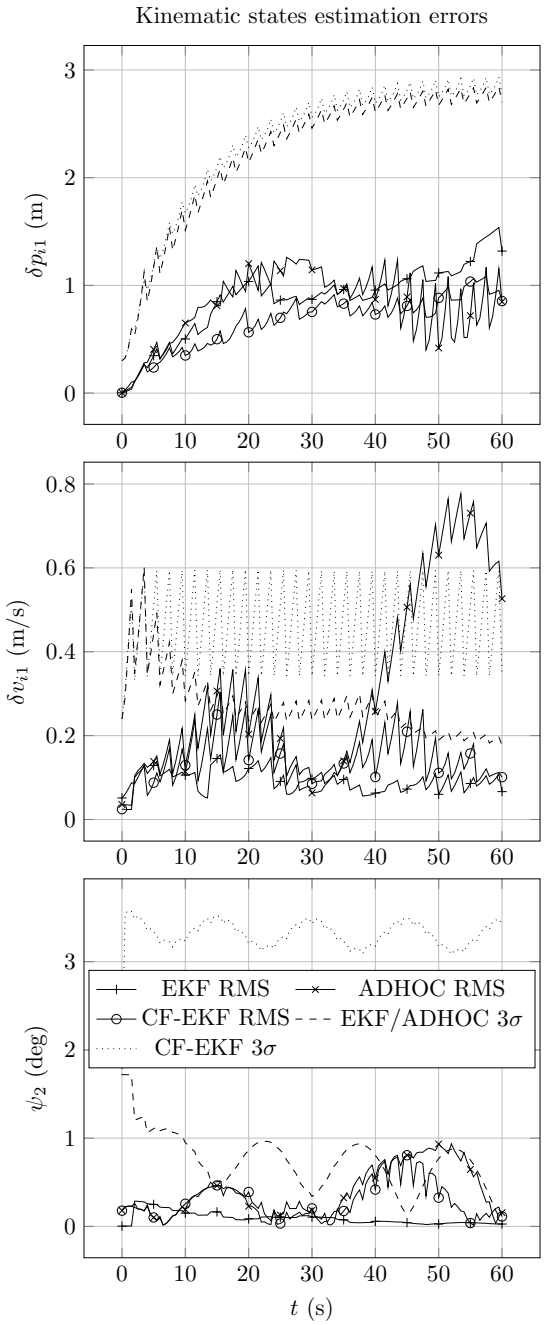

Fig. 4. Kinematics states error results.

Kalman filter statistical divergence (notice that RMS divergence is also observed). This precludes filter validation and usage. Suboptimal inflation of process noise could bring the filter back to statistical convergence, but the tuning strategy is often a blind and painful trial-and-error method which often yield poor overall performance. Similar performance patterns are observed in misalignment and accelerometer error curves.

Statistical inconsistency and RMS error divergence is also seen in *ad hoc* CF/EKF estimation of rate-gyro drift. Moreover, the trade-off in this component is observability: while this vehicle trajectory allows for drift observability in EKF, the CF-EKF does not react to it. Finally, none of the filters has magnetic bias observability.

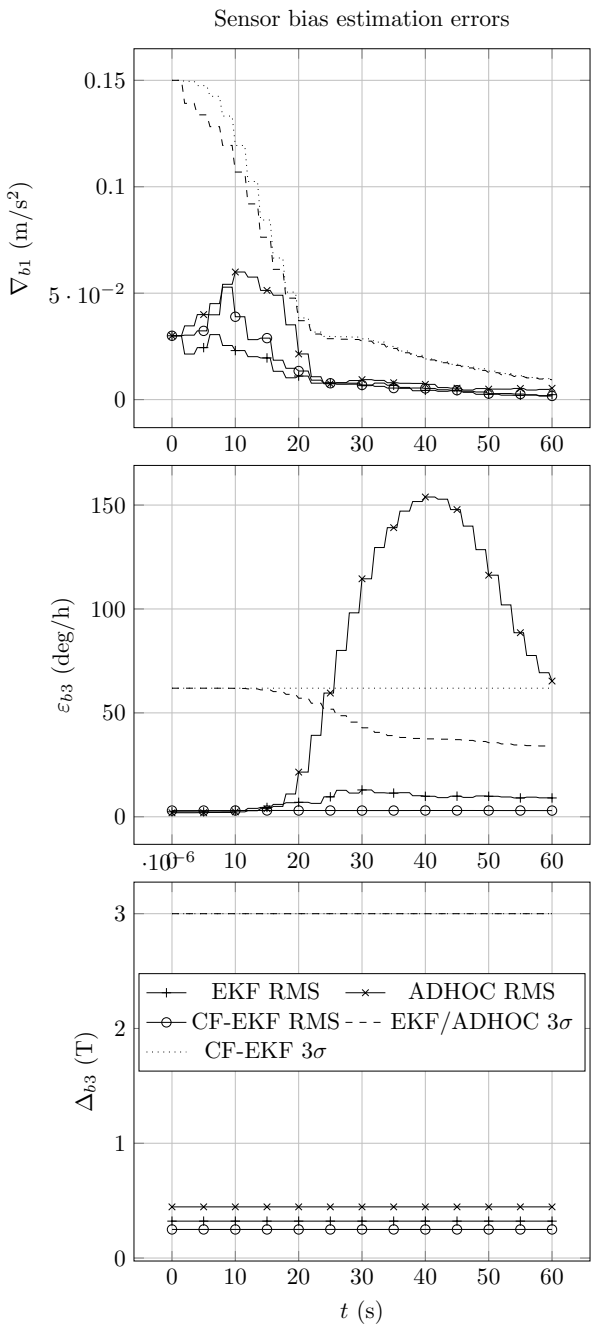

Fig. 5. Sensors bias states error results.

6. CONCLUSION

This paper laid the foundation for CF and EKF interfacing without imposing excessive suboptimal assumptions that often reduce performance and make it impracticable for tuning. While CF employed IMU/magnetometer measurements to bound attitude errors, an external EKF bounded position and velocity errors by means of CF output and GNSS measurements. Any other traditional EKF aiding sensor could be employed in the CF-EKF architecture as well.

The main feature of the CF-EKF algorithm is the possibility of deployment in a distributed multi-platform system. This paper showed how to implement fault isolation by running the CF stage in a separate low-throughput low-level reliable machine for CF stand-alone degraded mode operation. This allows for manual recovery of an auto-pilot failure due to a navigation system fault. Although the CF is simple enough to be directly implemented in a simple computing hardware, the EKF calls for high-order matrices inversion that are numerically expensive and unstable. Ongoing work investigates equivalent numerically more robust approaches to the classic EKF formulation (such as U-D factorization) for implementation in an embedded μUAV real-time computer [Lustosa et al. (2015)]. This will allow for proper assessment of its performance in more realistic conditions under real-time control system requirements (e.g., continuous position and velocity estimates).

REFERENCES

Bar-Shalom, Y., Li, X.R., and Kirubarajan, T. (2001). *Estimation with aapplication to tracking and navigation: theory, algorithms and software.* Wiley-Interscience.

Calusdian, J., Yun, X., and Bachmann, E. (2011). Adaptive-gain complementary filter of inertial and magnetic data for orientation estimation. In *Proc. IEEE/RSJ Int. Conf. Robot. Automat. (ICRA)*, 1916–1922.

Euston, M., Coote, P., Mahony, R., Kim, J., and Hamel, T. (2008). A complementary filter for attitude estimation of a fixed-wing uav. In *Proc. IEEE/RSJ Int. Conf. Intell. Robots Syst.*, 340–345.

Farrell, J.A. and Barth, M. (1998). *The global positioning system and inertial navigation.* McGraw-Hill.

Gordon, N.J., Salmond, D.J., and Smith, A.F.M. (1993). Novel approach to nonlinear/non-Gaussian Bayesian state estimation. *IEEE Proceedings F - Radar and Signal Processing*, 140(2), 107–113.

Goshen-Meskin, D. and Bar-Itzhack, I.Y. (1992). Observability analysis of piece-wise constant systems, ii. application to inertial navigation in-flight alignment. *IEEE Transactions on Aerospace and Electronic Systems*, 28(4), 1068–1075.

Higgins, W.T. (1975). A comparison of complementary and Kalman filtering. *IEEE Transactions on Aerospace and Electronic Systems*, AES-11(3), 321–325.

Jung, D. and Tsiotras, P. (2007). Inertial attitude and position reference system development for a small uav. In *In AIAA Infotech @ Aerospace 2007 Conference and Exhibit.*

Lustosa, L.R., Defay, F., and Moschetta, J.M. (2015). Longitudinal study of a tilt-body vehicle: modeling, control and stability analysis. In *Proc. Int. Conf. on Unmanned Aircraft Systems (ICUAS)*, 816–824.

Mahony, R., Hamel, T., and Pflimlin, J.M. (2005). Complementary filter design on the special orthogonal group so(3). In *Proc. IEEE Conf. Decision Control*, 1477–1484.

Maybeck, P.S. (1979). *Stochastic models, estimation, and control.* Academic Press.

Stevens, B.L. and Lewis, F.L. (2003). *Aircraft control and simulation.* Wiley-Interscience.

Vasconcelos, J.F., Silvestre, C., Oliveira, P., Batista, P., and Cardeira, B. (2009). Discrete time-varying attitude complementary filter. In *Proc. American Control Conference*, 4056–4061.